Bioorganic & Medicinal Chemistry Letters 22 (2012) 980–984

Contents lists available at SciVerse ScienceDirect

Bioorganic & Medicinal Chemistry Letters

journal homepage: www.elsevier.com/locate/bmcl

Discovery of potent and liver-targeted stearoyl-CoA desaturase (SCD) inhibitors in a bispyrrolidine series

Nicolas Lachance [a,*], Yves Gareau [a], Sébastien Guiral [b], Zheng Huang [b], Elise Isabel [a], Jean-Philippe Leclerc [a], Serge Léger [a], Evelyn Martins [a], Christian Nadeau [c], Renata M. Oballa [a], Stéphane G. Ouellet [c], David A. Powell [a], Yeeman K. Ramtohul [a], Geoffrey K. Tranmer [a], Thao Trinh [c], Hao Wang [b], Lei Zhang [b]

[a] Department of Medicinal Chemistry, Merck Frosst Centre for Therapeutic Research, 16711 TransCanada Hwy, Kirkland, Quebec, Canada H9H 3L1
[b] Department of Biochemistry and Molecular Biology, Merck Frosst Centre for Therapeutic Research, 16711 TransCanada Hwy, Kirkland, Quebec, Canada H9H 3L1
[c] Department of Basic Pharmaceutical Sciences, Merck Frosst Centre for Therapeutic Research, 16711 TransCanada Hwy, Kirkland, Quebec, Canada H9H 3L1

ARTICLE INFO

Article history:
Received 31 October 2011
Revised 30 November 2011
Accepted 1 December 2011
Available online 8 December 2011

Keywords:
Stearoyl-CoA desaturase inhibitors
SCD inhibitors
Desaturation index
Liver-targeted
MK-8245

ABSTRACT

Inhibition of stearoyl-CoA desaturase (SCD) activity represents a potential novel mechanism for the treatment of metabolic disorders including obesity and type II diabetes. To circumvent skin and eye adverse events observed in rodents with systemically-distributed SCD inhibitors, our research efforts have been focused on the search for new and structurally diverse liver-targeted SCD inhibitors. This work has led to the discovery of novel, potent and structurally diverse liver-targeted bispyrrolidine SCD inhibitors. These compounds possess suitable cellular activity and pharmacokinetic properties to inhibit liver SCD activity in a mouse pharmacodynamic model.

Elevated stearoyl-CoA desaturase (SCD) activity has been linked to a number of metabolic disorders including obesity and type II diabetes, which continue to expand at epidemic rates.[1] The SCD enzyme exists as two isoforms in humans (SCD1 and SCD5) and four in rodents (SCD1-4), with SCD1 being the isoform which is predominantly expressed in liver (target organ for efficacy). It has been reported that adverse events (AEs),[2] such as partial eye closure and progressive alopecia, appear in mice after ~7 days of treatment with systemically-distributed SCD inhibitors. These AEs are likely due to the depletion of SCD-derived lubricating lipids in skin and eye, and it was initially hypothesized that liver-targeted SCD inhibitors should circumvent these issues.[3]

The initial strategy employed in the design of liver-selective compounds centers on exploring the addition of polar acidic moieties which are recognized by organic anionic transporters (OATPs),[4] such as tetrazoles or carboxylic acids, on SCD inhibitors to obtain the desired in vivo properties: a high liver concentration (target organ for efficacy) and a low systemic concentration to minimize exposures in off-target tissues and cells associated with adverse events (skin and eye).

We recently disclosed MK-8245 (Fig. 1), a phenoxy piperidine isoxazole derivative, as a potent and liver-selective SCD inhibitor with an enzymatic potency (IC_{50}) against the rat SCD of 3 nM.[5] This compound possesses good in vivo potency in a mouse liver pharmacodynamic model (mLPD, ED_{50} ~1 mg/kg).[6] Moreover, MK-8245 demonstrated a therapeutic window for liver-lipid efficacy in the absence of AEs after 4 weeks of chronic dosing in mice.[5] Following the discovery of MK-8245, our research efforts continued on the identification of structurally diverse liver-targeted SCD inhibitors for the selection of a back-up compound to our lead MK-8245 to support the development of SCD inhibitors in preclinical species and eventually in humans.[7]

In vitro studies have demonstrated that the liver-targeted tissue distribution profile of MK-8245 is likely a result of substrate recognition by organic anionic transporter proteins (OATPs) which are highly expressed in hepatocytes.[4,5] An important feature in the structure of MK-8245 is the tetrazole acetic acid moiety, which is the key functionality for OATP recognition. In search for new structural classes, we intentionally kept this group in place for active transporter recognition and modified other parts of the molecule. We envisioned that replacement of the piperidine core in MK-8245, which is commonly found in many SCD-inhibitors,[2a,8] with linkers such as a bicyclic heterocycles (A–B) may provide a distinct and structurally diverse series of SCD1 inhibitors **1** (Fig. 1).[9,10]

In the absence of an SCD1 enzyme X-ray crystal structure, we chose to proceed with a systematic SAR study to guide our optimization efforts. Initially, we turned our attention to the synthesis of

* Corresponding author.
E-mail address: nicolas.lachance21@gmail.com (N. Lachance).

0960-894X/$ - see front matter © 2011 Elsevier Ltd. All rights reserved.
doi:10.1016/j.bmcl.2011.12.002

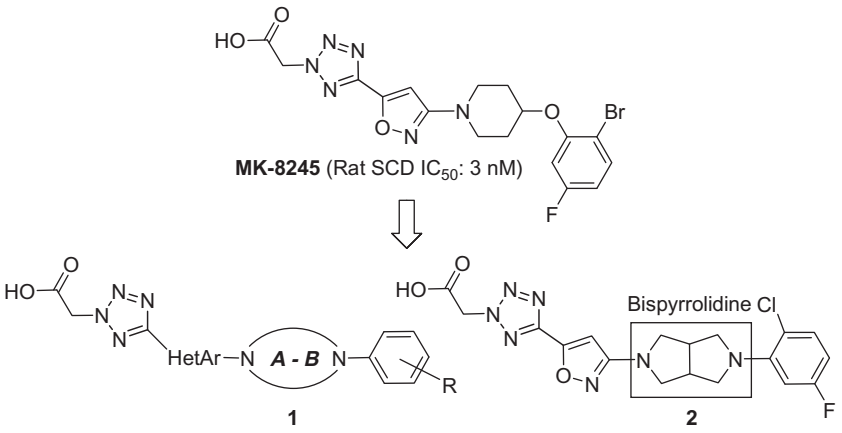

Figure 1. MK-8245, core structure of heterocyclic linkers **1** and bispyrrolidine compound **2**.

the bispyrrolidine linker **2** (Fig. 1) while keeping the remaining structural elements of MK-8245 almost unchanged. The bromine atom on the phenyl ring was substituted by a chlorine atom to simplify the synthetic route (Scheme 1).

As depicted in Scheme 1, the construction of heterocyclic linker counterparts **5** involved the Buchwald–Hartwig amination of aryl bromide **4** with amino heterocycle **3** in the presence of a base (NaO*t*-Bu) and a catalytic amount of $Pd(OAc)_2$ and (±)-BINAP.[9,11] The *N*-Boc protecting group was then cleaved under acidic conditions with HCl or TFA to form the corresponding salt **5**.

Having in hand a suitable collection of linkers **5** derived from different heterocyclic linkers (A–B) **3**, we next turned our attention to join these molecules to the isoxazole tetrazole acetic acid moiety. As illustrated in Scheme 2, the synthetic route consisted of a stepwise construction of the tetrazole acetic acid group. To this end, reaction of 3-bromoisoxazoline **6** with **5a** under addition–elimination conditions with Na_2CO_3 gave the corresponding product **7**.[12] The isoxazoline **7** thus obtained was conveniently oxidized to the desired isoxazole **8** with I_2 in presence of imidazole.[12] The preparation of the tetrazole **9** was completed by dehydration of amide **8** with TFAA to the corresponding nitrile followed by reaction with NaN_3 under slightly acidic conditions. Introduction of the acetate ester group on the tetrazole **9** gave two regioisomers **10** and **11**. It was observed that under Et_3N and THF conditions, a good ratio (>3:1) in favor of **10** could be obtained.[13] Finally, hydrolysis of **10** with aqueous formic acid afforded **2**.

We rapidly realized that the connection of a broad range of heterocyclic linkers **5** with the isoxazole aromatic core contained in MK-8245 would require a repetitive tedious synthesis of the tetrazole acetic acid moiety, as well as the oxidation step of the isoxazoline to the isoxazole aromatic ring for each analog. For synthetic ease, we decided to explore the replacement of the isoxazole ring with other five-membered heterocycles before evaluating other heterocyclic linkers (A–B) contained in **5**.

As reported in Scheme 3, a flexible route for the synthesis of thiazole **18** and thiadiazole **19** (Table 1) was developed through the use of a highly functionalized intermediate **16**. Compounds **18** and **19** were prepared via displacement of a bromo-heterocycle **16** with an appropriately substituted phenyl heterocyclic linker **5**, followed by cleavage of the ester group under either basic or acidic conditions. The versatile synthetic intermediate **16** was accessed through the elaboration of the tetrazole acetic acid group from the nitrile **14** by employing similar conditions as described for the isoxazoles **2** (Scheme 2). Following literature conditions,[9] the nitrile intermediate **14** was prepared from the thiazole **12** or the thiadiazole **13**. In addition, employing this route for thiazole **18** and thiadiazole **19** represented an expedient method that also allows the preparation of heterocycle targets **20–25** in only two steps.

The SCD inhibitors prepared were tested against the SCD1 enzyme in an SCD-induced rat liver microsomal assay.[14] Their cellular potencies were evaluated in a human hepatocellular carcinoma

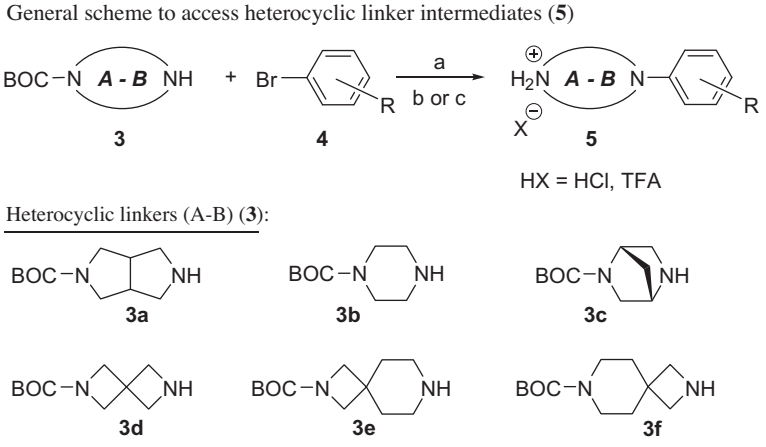

Scheme 1. Preparation of intermediates **5**. Reagents and conditions: (a) Sealed tube: $Pd(OAc)_2$, (±)-BINAP, NaO*t*-Bu, toluene, 115–120 °C for 16 h; (b) 2.0 M HCl in 1,4-dioxane, rt for 2 h; (c) TFA, CH_2Cl_2, rt for 1 h.

Synthesis of bispyrrolidine isoxazole compound (**2**)

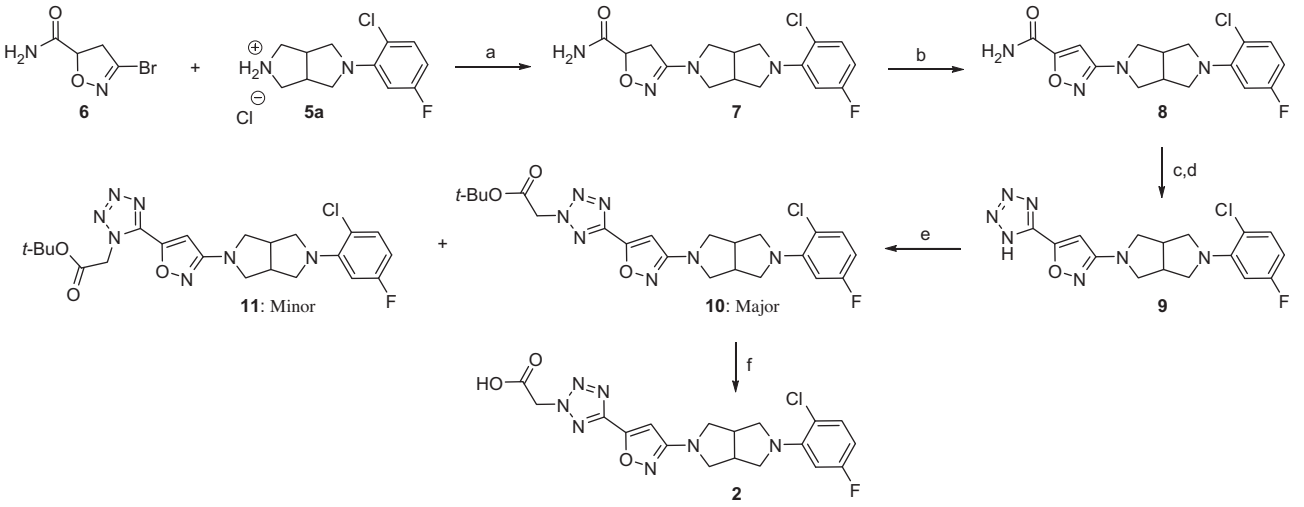

Scheme 2. Preparation of bispyrrolidine **2**. Reagents and conditions: (a) Na_2CO_3, *n*-BuOH, 110 °C for 16 h; (b) I_2, imidazole, toluene, reflux for 16 h; (c) TFAA, Et_3N, THF, 0 °C to rt for 1 h; (d) NaN_3, NH_4Cl, DMSO, 1,4-dioxane, 110 °C for 16 h; (e) *t*-butyl bromoacetate, Et_3N, THF, 80 °C for 1 h; (f) 85–90% aq HCO_2H, 100 °C for 1 h.

General route to heterocyclic compounds (**18-25**)

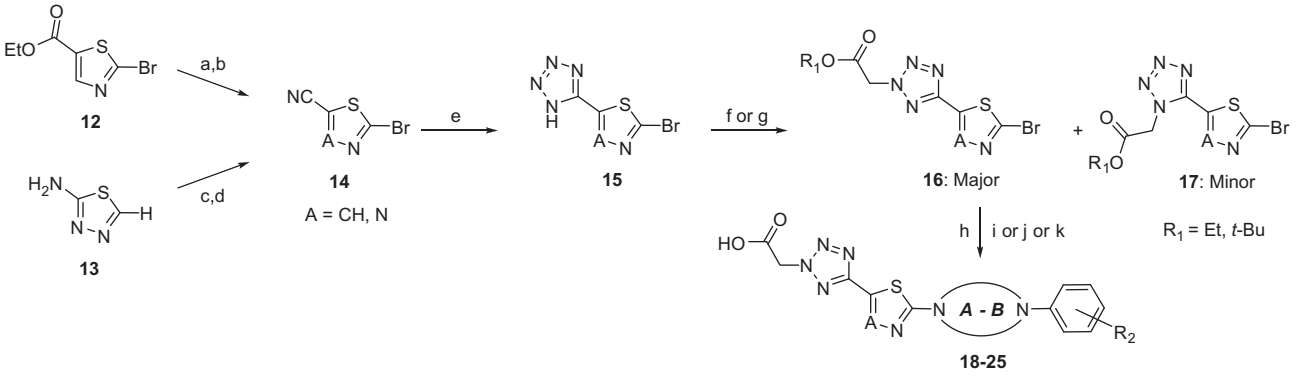

Scheme 3. Preparation of analogs in Tables 1 and 2. Reagents and conditions: (a) NH_4OH, MeOH, THF, rt for 4 h; (b) TFAA, Et_3N, THF, 0 °C to rt for 2 h; (c) Br_2, NaOAc, concd AcOH, rt for 3 h; (d) CuCN, *t*-butyl nitrite, MeCN, 0 °C to rt for 1 h; (e) Sealed tube: NaN_3, $ZnBr_2$, H_2O, *i*-PrOH, 120 °C for 5–16 h; (f) (A = CH): ethyl bromoacetate or *t*-butyl bromoacetate, Et_3N, THF, 80 °C for 1 h; (g) (A = N): ethyl bromoacetate, $CsCO_3$, DMF, 90 °C for 1 h; (h) **5**, DBU or Hünig's base, NMP, 120–130 °C for 20–30 min; (i) 1 N LiOH, MeOH, THF, rt for 1 h; (j) TFA, CH_2Cl_2, rt for 4 h; (k) 85–90% aq HCO_2H, 100 °C for 1 h.

line (HepG2) as the whole cell assay in which cells are devoid of active OATPs.[15] The ability to cross the cell membrane through active transporters was assessed in a rat hepatocyte (Rat Hep) assay which contains functional OATPs.[5] The purpose was to qualitatively determine if an SCD inhibitor was actively transported into hepatocytes (potent Rat Hep IC_{50}) while maintaining poor cell permeability (poor HepG2 IC_{50}) to avoid passive diffusion into off-target cells.

As shown in Table 1 across the bispyrrolidine analogs **2**, **18** and **19**, the optimal heterocycle is the isoxazole ring, but the thiazole ring is quite comparable.[16] The isoxazoyl bispyrrolidine **2** displayed a ~400-fold potency shift between the microsomal enzyme assay (Rat SCD) and the HepG2 cellular assay (IC_{50} = 9900 nM) but improved to 8-fold in the rat hepatocyte cellular assay (IC_{50} = 198 nM), which suggests recognition by active transporters. Overall, the bispyrrolidine **2** showed 3 to 9-fold reduced in vitro potency (Rat SCD, HepG2 and Rat Hep) when compared to MK-8245 (Table 1).

The enzymatic potency against the human SCD enzyme was also measured. In a human SCD1 enzyme assay (hSCD1) (delta-9 desaturase), compound **2** displayed an IC_{50} of 27 nM compared to 1 nM for MK-8245.[5] The bispyrrolidine linker **2** is slightly less potent at inhibiting the other isoform found in human (hSCD5 IC_{50} = 242 nM).[17] In addition, it is selective over two other desaturase enzymes (delta-5 and delta-6 desaturases) present in human, with IC_{50}s >80 μM in a whole cell assay.[15]

Before pursuing further SAR, we decided to evaluate the in vivo potency of **2** in a mouse liver pharmacodynamic model (mLPD).[6] To support this model, the activity for the bispyrrolidine **2** was measured in a mouse SCD1 enzyme assay (IC_{50} = 18 nM) which showed a similar potency compared to the rat SCD enzyme. Also, the dose selection was based on the pharmacokinetic (PK) profile determined in C57BL6 mice following oral dosing at 10 mg/kg in 0.5% methocel as the vehicle. Under these conditions, the bispyrrolidine **2** had a reasonable liver concentration of 2.7 μM at a 6 h time-point (F = 24%, AUC_{0-6h} = 2.1 μM h). Consequently, a moderate dose (10 mg/kg) of **2** was enough to efficiently suppress liver SCD activity in the mLPD assay (72% inhibition at a liver concentration of 14.8 μM of **2** at a 3 h time-point). In contrast, the more potent MK-8245 required a lower

Table 1
SAR on the heteroaromatic ring

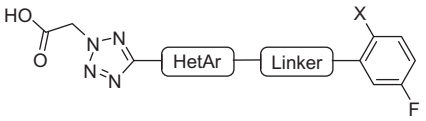

Compound	HetAr-linker	X	IC_{50}[a] (nM)		
			Rat SCD	HepG2	Rat Hep
MK-8245	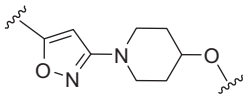	Br	3	1070	68
2	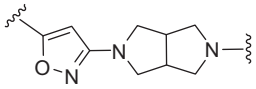	Cl	24	9900	198
18	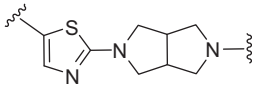	Cl	34	15,400	233
19	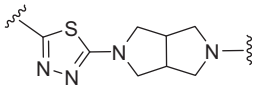	Cl	59	>10,000	300

[a] IC_{50}s are average of at least two independent titrations.

Table 2
SAR on the heterocyclic linker

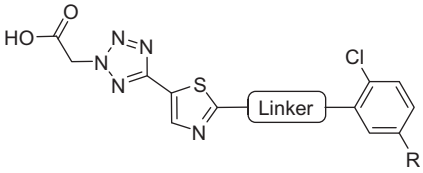

Compound	Linker	R	IC_{50} (nM)		
			Rat SCD	HepG2	Rat Hep
20	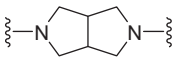	OCF_3	9	2450	113
21	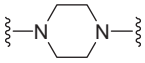	F	28	4200	134
22		F	29	9140	176
23	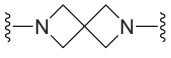	F	43	50,900	103
24		F	128	>100,000	506
25		F	36	>100,000	438

dose of 2 mg/kg in the mLPD model to afford 89% liver SCD inhibition at a liver exposure of 4.9 μM.

Despite a good liver exposure of **2** in mice, the moderate in vivo activity of **2** in mLPD oriented our synthetic efforts on improving the in vivo potency by increasing the overall in vitro SCD-activity of this class of inhibitors.

Since the bispyrrolidine core contained in **2** was the first replacement explored and the fact that the thiazole is a good replacement for the isoxazole ring, we pursued further SAR exploration through evaluation of a broad range of heterocyclic linkers (A–B) (Table 2). The rapid preparation of these analogs **21**–**25** relied on the convenient two steps coupling of phenyl heterocyclic linkers **5** with the key thiazole intermediate **16** (Scheme 3).

The activities on the SCD-induced rat liver microsomal assay for the heterocycles **21–25** prepared are reported in Table 2. Interestingly, SCD inhibitory activity (HepG2 and Rat Hep) was slightly improved with the piperazine tether **21**. However, the spiro linkers **23**–**25** were intrinsically less potent. Having in hand two good replacements for the piperidine core, namely the bispyrrolidine and the piperazine, we turned our attention to the SAR on the phenyl moiety in both series. Among the many substituents explored,[18] we found that the phenyl ring substituted with an OCF_3 group instead of the fluorine improved the in vitro potency of **20** when compared to **18** (Tables 1 and 2). However with compound **21**, the current chlorine–fluorine substitution pattern on the phenyl ring appeared optimal.[18]

For comparison to **2**, PK profiles were measured for the thiazoles **20** and **21** in C57BL6 mice following a typical 10 mg/kg oral dosing (**20**: $F = 38\%$, $AUC_{0-6h} = 1.5$ μM h; **21**: $F = 15\%$, $AUC_{0-6h} = 0.7$ μM h). Gratifyingly, the liver concentrations at a 6 h timepoint (**20**: 21.3 μM; **21**: 9.3 μM) were significantly improved. Evaluation of the bispyrrolidine **20** in the mLPD model showed a 76% inhibition at a lower dose of 2 mg/kg with a liver exposure of 23.2 μM, whereas the piperazine **21** exhibited a 61% inhibition at the same dose with a liver exposure of 7.7 μM (total drug concentration, see Table 3).[19] In summary, the bispyrrolidine **20** and the piperazine **21** possess good in vitro potency and good in vivo inhibition of liver SCD activity in the mLPD at 2 mg/kg (Table 3).[20]

As expected, **20** and **21** displayed a liver-selective tissue distribution profile. The mouse liver/plasma (L/P) ratios (**20**: 60-fold; **21**: 40-fold) were slightly reduced up to two folds and the liver/Harderian glands (L/H) ratios (**20**: 40-fold; **21**: 180-fold) were improved when compared to MK-8245 (L/P: 90-fold; L/H: 20-fold) (Table 3). This good tissue-selectivity for the liver organ is desirable, given the connection that inhibiting SCD in the Harderian glands is associated with eye AEs.[5]

Table 3
In vitro and in vivo profiles of MK-8245, **20** and **21** in mice

	Mouse SCD	In vivo	
	IC_{50} (nM)	TD[a] (μM)	mLPD[b]
MK-8245	3	[Liver] = 2.7 [Plasma] = 0.03 [Harderian glands] = 0.13	89% inh. at 2 mg/kg [Liver] = 4.9 μM 49% inh. at 0.4 mg/kg [Liver] = 1.6 μM
20	9	[Liver] = 21.3 [Plasma] = 0.36 [Harderian glands] = 0.51	76% inh. at 2 mg/kg [Liver] = 23.2 μM
21	21	[Liver] = 9.3 [Plasma] = 0.22 [Harderian glands] = 0.05	61% inh. at 2 mg/kg [Liver] = 7.7 μM

[a] TD—tissue distribution (PO, mouse (n = 2), 10 mg/kg; 6 h post dose).
[b] mLPD (PO, mouse (n = 5), 3 h post dose); inh.—inhibition.

In conclusion, we have identified a bispyrrolidine and a piperazine series as new structural motifs for SCD inhibitors. In these series, the piperidine core present in MK-8245, and in other common SCD-inhibitors,[8] is replaced by moderately rigid heterocycles connecting the thiazole or isoxazole ring with the phenyl ring via a C–N bond. SAR around the bispyrrolidine core led to the identification of the thiazole heterocycle and the 2-chloro-5-trifluoromethoxyphenyl in **20**, as an excellent combination for both in vitro potency and in vivo efficacy. Presently, the exploration of the bispyrrolidine series is suspended but any future work will need to focus on improving mLPD activity in this series by increasing in vitro inhibitory activity for Rat SCD and Rat Hep assays, and to evaluate the therapeutic profile in a 4-week chronic dosing model.

Acknowledgments

The authors thank Dan Sørensen for NMR spectroscopic assistance on gHMBC, ^{15}N gHMBC and 1D NOESY experiments.

References and notes

1. Reviews: (a) Dobrzyn, P.; Dobrzyn, A. *Expert Opin. Ther. Patents* **2010**, *20*, 849 and references cited therein; (b) Liu, G. *Expert Opin. Ther. Patents* **2009**, *19*, 1169 and references cited therein.
2. Leading references: (Mice AEs): (a) Leger, S.; Black, C.; Deschenes, D.; Dolman, S.; Falgueyret, J.-P.; Gagnon, M.; Guiral, S.; Huang, Z.; Guay, J.; Leblanc, Y.; Li, C.-S.; Masse, F.; Oballa, R.; Zhang, L. *Bioorg. Med. Chem. Lett.* **2010**, *20*, 499; (b) Ramtohul, Y. K.; Black, C.; Chan, C.-C.; Crane, S.; Guay, J.; Guiral, S.; Huang, Z.; Oballa, R.; Xu, L.-J.; Zhang, L.; Li, C. S. *Bioorg. Med. Chem. Lett.* **2010**, *20*, 1593; (c) Li, C. S.; Belair, L.; Guay, J.; Murgasva, R.; Sturkenboom, W.; Ramtohul, Y. K.; Zhang, L.; Huang, Z. *Bioorg. Med. Chem. Lett.* **2009**, *19*, 5214. (Rats AEs): (d) Atkinson, K. A.; Beretta, E. E.; Brown, J. A.; Castrodad, M.; Chen, Y.; Cosgrove, J. M.; Du, P.; Litchfield, J.; Makowski, M.; Martin, K.; McLellan, T. J.; Neagu, C.; Perry, D. A.; Piotrowski, D. W.; Steppan, C. M.; Trilles, R. *Bioorg. Med. Chem. Lett.* **2011**, *21*, 1621.
3. (a) Ramtohul, Y. K.; Powell, D.; Leclerc, J.-P.; Leger, S.; Oballa, R.; Black, C.; Isabel, E.; Li, C. S.; Crane, S.; Robichaud, J.; Guay, J.; Guiral, S.; Zhang, L.; Huang, Z. *Bioorg. Med. Chem. Lett.* **2011**, *21*, 5692; (b) Uto, Y.; Ueno, Y.; Kiyotsuka, Y.; Miyazawa, Y.; Kurata, H.; Ogata, T.; Yamada, M.; Deguchi, T.; Konishi, M.; Takagi, T.; Wakimoto, S.; Ohsumi, J. *Eur. J. Med. Chem.* **2010**, *45*, 4788 and references cited therein; (c) Uto, Y.; Ogata, T.; Kiyotsuka, Y.; Ueno, Y.; Miyazawa, Y.; Kurata, H.; Deguchi, T.; Watanabe, N.; Konishi, M.; Okuyama, R.; Kurikawa, N.; Takagi, T.; Wakimoto, S.; Ohsumi, J. *Bioorg. Med. Chem. Lett.* **2010**, *20*, 341; (d) Koltun, D. O.; Vasilevich, N. I.; Parkhill, E. Q.; Glushkov, A. I.; Zilbershtein, T. M.; Mayboroda, E. I.; Boze, M. A.; Cole, A. G.; Henderson, I.; Zautke, N. A.; Brunn, S. A.; Chu, N.; Hao, J.; Mollova, N.; Leung, K.; Chisholm, J. W.; Zablocki, J. *Bioorg. Med. Chem. Lett.* **2009**, *19*, 3050 and references cited therein.
4. Review on OATPs: Niemi, M. *Pharmacogenomics* **2007**, *8*, 787.
5. Oballa, R. M.; Belair, L.; Black, W. C.; Bleasby, K.; Chan, C. C.; Desroches, C.; Du, X.; Gordon, R.; Guay, J.; Guiral, S.; Hafey, M. J.; Hamelin, E.; Huang, Z.; Kennedy, B.; Lachance, N.; Landry, F.; Li, C. S.; Mancini, J.; Normandin, D.; Pocai, A.; Powell, D. A.; Ramtohul, Y. K.; Skorey, K.; Sørensen, D.; Sturkenboom, W.; Styhler, A.; Waddleton, D. M.; Wang, H.; Wong, S.; Xu, L.; Zhang, L. *J. Med. Chem.* **2011**, *54*, 5082.
6. Mouse liver pharmacodynamic model (mLPD) is expressed in percentage (%) inhibition and is used to assess the in vivo potency. In the mLPD experiment, mice were fed on a high carbohydrate diet and the SCD activity was indexed 3 h post oral dose of SCD inhibitors by following the conversion of intravenously administered [1-^{14}C]-stearic acid tracer to the SCD-derived [1-^{14}C]-oleic acid in liver lipids. The percentage (%) of inhibition of an SCD inhibitor is calculated from the liver SCD activity index (ratio of ^{14}C-oleic acid/^{14}C-stearic acid) from drug treated animals compared to a vehicle group.
7. Lachance, N.; Guiral, S.; Huang, Z.; Leclerc, J.-P.; Li, C. S.; Oballa, R. M.; Ramtohul, Y. K.; Wang, H.; Wu, J.; Zhang, L. *Bioorg. Med. Chem. Lett.* **2011**. doi:10.1016/j.bmcl.2011.10.070.
8. Leading references: (a) Zhao, H.; Serby, M. D.; Smith, H. T.; Cao, N.; Suhar, T. S.; Surowy, T. K.; Camp, H. S.; Collins, C. A.; Sham, H. L.; Liu, G. *Bioorg. Med. Chem. Lett.* **2007**, *17*, 3388; (b) Liu, G.; Lynch, J. K.; Freeman, J.; Liu, B.; Xin, Z.; Zhao, H.; Serby, M. D.; Kym, P. R.; Suhar, T. S.; Smith, H. T.; Cao, N.; Yang, R.; Janis, R. S.; Krauser, J. A.; Cepa, S. P.; Beno, D. W. A.; Sham, H. L.; Collins, C. A.; Surowy, T. K.; Camp, H. S. *J. Med. Chem.* **2007**, *50*, 3086.
9. Detailed experimental procedures: Lachance, N.; Leger, S.; Oballa, R. M.; Powell, D.; Tranmer, G. K.; Martins, E.; Gareau, Y. WO 2010/108268 and references cited therein.
10. (a) During the course of this study, three separate patent applications describing new systemically-distributed SCD inhibitors containing bicyclic heterocycles tether were published: Zoller, G.; Voss, M. D.; Matter, H.; Herling, A. WO 2010/028761.; (b) Chaudhari, S. S.; Thomas, A.; Gudade, G. B.; Kadam, A.; Patil, N. P.; Khairatkar-Joshi, N.; Shah, D. M. WO 2009/037542.; (c) Zoller, G.; Voss, M. D.; Keil, S.; Herling, A.; Matter, H. WO 2008/135141.
11. Wolfe, J. P.; Buchwald, S. L. *J. Org. Chem.* **2000**, *65*, 1144 and references cited therein.
12. Girardin, M.; Alsabeh, P. G.; Lauzon, S.; Dolman, S. J.; Ouellet, S. G.; Hughes, G. *Org. Lett.* **2009**, *11*, 1159.
13. The regiochemistry of the acetic acid side chain on the tetrazole was confirmed by evaluation of the structures through NMR experiments: gHMBC, ^{15}N gHMBC and 1D NOESY.
14. Rat microsomal assay conditions: Li, C. S.; Ramtohul, Y.; Huang, Z.; Lachance, N. WO 2006/130986.
15. Zhang, L.; Ramtohul, Y.; Gagné, S.; Styhler, A.; Guay, J.; Huang, Z. *J. Biomol. Screen.* **2010**, *15*, 169.
16. Compounds containing a six-membered heterocycle ring pyrimidine were less potent. Data unpublished.
17. Powell, D. A.; Ramtohul, Y.; Lebrun, M.-E.; Oballa, R.; Bhat, S.; Falgueyret, J.-P.; Guiral, S.; Huang, Z.; Skorey, K.; Tawa, P.; Zhang, L. *Bioorg. Med. Chem. Lett.* **2010**, *20*, 6366.
18. Several substituents (F, Cl, Br, Me, CF_3, SO_2Me, OMe, OEt, OCH_2Cyp, Ph) were evaluated across numerous combination at the *ortho*, *meta* and *para* positions on the phenyl ring. Unpublished results.
19. The available or free drug concentration in the liver homogenate was not measured for compounds **20** and **21**. Total drug concentration presented in Table 3 supports the efficacy of MK-8245, **20** and **21** in mLPD.
20. MK-8245, **20**, **21** were tested in three separate mLPD experiments; n = 5 mice per group. A difference (10–15%) of inhibitory activity from 61% to 76% or from 76% to 89% in the mLPD is not statistically significant.